APPLIED AND ENVIRONMENTAL MICROBIOLOGY, June 1981, p. 1442-1453
0099-2240/81/061442-12$02.00/0

Vol. 41, No. 6

Effect of Manual Brush Cleaning on Biomass and Community Structure of Microfouling Film Formed on Aluminum and Titanium Surfaces Exposed to Rapidly Flowing Seawater

JANET S. NICKELS,[1] RONALD J. BOBBIE,[1] DAN F. LOTT,[2] ROBERT F. MARTZ,[1] PETER H. BENSON,[3] AND DAVID C. WHITE[1]*

Department of Biological Science, Florida State University, Tallahassee, Florida 32306[1]; Naval Coastal Systems Center, Panama City, Florida 32407[2]; and Argonne National Laboratory, Argonne, Illinois 60439[3]

Received 22 December 1980/Accepted 19 March 1981

Metals exposed to rapidly flowing seawater are fouled by microbes that increase heat transfer resistance. In this study, results of biochemical test methods quantitatively relating the biomass and community structure of the microfouling film on aluminum and titanium to heat transfer resistance across the metal surface during three cycles of free fouling and manual brushing showed that cleaning accelerates the rate of fouling measured as the loss of heat transfer efficiency and as microfouling film biomass. The results also showed that the rate of fouling, measured as an increase in heat transfer resistance, is faster on titanium than on aluminum but that the titanium surface is more readily cleaned. In three cycles of free fouling and cleaning with a stiff-bristle nylon brush, the free-fouling communities re-forming on aluminum became enriched in bacteria containing short-branched fatty acids as the cycling progressed. The free-fouling community on titanium revealed an increasingly diverse morphology under scanning electron microscopy that was enriched in a portion of the microeucaryotes. Brushing removed most of the biomass, but left a residual community that was relatively enriched in a portion of the bacterial assembly containing cyclopropane fatty acids on aluminum and in a more diverse community on the titanium surface. The residual communities left after cleaning of titanium revealed an increase in bacteria with short-branched fatty acids and in microeucaryotes as cleaning continued. No significant changes occurred in the residual microbial community structure left on aluminum with cleaning; it was, again, less diverse than that remaining on titanium. The residual communities secreted a twofold-larger amount of extracellular polymer, measured as the ratio of total organic carbon to lipid phosphate, than did the free-fouling community on both surfaces.

The fouling of metal surfaces exposed to seawater has serious consequences for the utilization, by ocean thermal energy conversion (OTEC) systems, of temperature differences between warm surface water and cold deep water of tropical oceans. A thin microbial biofouling film increases heat transfer resistance sufficiently to prevent utilization of this vast source of renewable energy (9). In addition, the microfouling film can complicate ecological experiments by concentrating a nutrient source on the seawater side of enclosures and lead to "bottle" effects. Consequently, it is important to study practical ways to control microfouling film formation.

Previous work has established the following sequence of events in the fouling of surfaces immersed in seawater. The initial event involves the immediate coating of the surface by biopolymers produced by organisms living in the sea; this film attracts microbes that first bind reversibly then irreversibly to the surface (7, 10, 15, 24) and form an acid polysaccharide extracellular polymeric film (13). The microbial fouling film then attracts a diverse microeucaryotic fouling population (6, 12, 14, 16), and, finally, macrofouling by larger eucaryotes occurs.

Because of the problem of increased heat transfer resistance caused by these microfouling films, methods that could quantitatively describe the biomass, physiological state, and community structure of the film were needed to determine and assess adequate control measures.

A suite of assays developed for examination of the estuarine detrital microbiota (3, 18-21, 23) was adapted to the analysis of the microfouling film in OTEC samples. Pipe sections were re-

moved from the flowing seawater for analysis of total organic carbon (TOC), examination of morphology by scanning electron microscopy, and lipid analysis after extraction of the film. From the lipid portion of the extract, the total cellular biomass (measured as the extractable lipid phosphate) was determined. Measurement of extractable lipid phosphate has been shown to correlate well with other measures of microbial biomass, such as adenosine triphosphate, muramic acid, enzyme and respiratory activities and the rates of thymidine incorporation into DNA and of lipid synthesis, and $^{14}CO_2$ release from various substrates (17–19).

From the water phase of the lipid extraction, the adenosine nucleotides can be recovered quantitatively and measured by fluorescence after specific derivatization with chloroacetaldehyde and analyzed by high-pressure liquid chromatography. The resiliency of the adenosine energy charge of the microfouling film to anoxia has been demonstrated with this method (8).

The major portion of the lipid fraction can then be subjected to mild acid methanolysis, and various components of the lipids can be fractionated by thin-layer chromatography, recovered, and analyzed by gas-liquid chromatography (3). This analysis of biomass and community structure correlates the morphology of detrital microbiota modified by addition of antibiotics and nutrients (as determined by scanning electron microscopy) with analyses of mixtures of microbial monocultures and of individual organisms cultured from detritus (20). The specific predation of the sand dollar *Mellita quinquiesperforata* on the benthic microbiota measured with these methods agreed with the induced changes expected from their known feeding habits (22).

With this background, the correlation of heat transfer resistance to the biomass and the community structure of the microfouling film after manual brush cleaning cycles was examined.

MATERIALS AND METHODS

Materials. All solvents were glass distilled (Burdick and Jackson, Muskegon, Mich.). Chloroform was glass distilled just before use. Other materials were described previously (3, 8, 21).

Exposure to seawater. Titanium and 5052 aluminum pipes (internal diameter, 2.66 cm [1-in. nominal]) were exposed to seawater flowing at 1.85 m/s (6 ft/s) at the Naval Coastal Systems Center, Panama City, Fla. (30°09'54" N, 85°15'32" W) between 19 September and 5 December 1979. This nutrient-rich nearshore site was chosen to accelerate microfouling changes. Microfouling from an open ocean thermal energy conversion site could be quantitatively as well as qualitatively different. Characteristics of the seawater at the intake point are given in Table 1. The falling temperatures in the later portion of the test period corresponded with a decrease by half in NH_3, NO_3, phosphate, and silicate and with smaller decreases in water column TOC and biological oxygen demand.

Test surfaces were exposed to seawater that was pumped from approximately 2 m below the surface of the bay into a 2,840-liter fiber glass feed tank and then through the heat transfer measuring units and the sample pipe sections. Heat transfer coefficient measurements were made as previously described (4, 11). At points B, E, and H (Fig. 1), the inside of the entire pipe was brushed with 20 passes of a stiff-bristle nylon bottle brush that tightly fit in the pipe. At time indicated by points C, F, and I (Fig. 1), duplicate prescored sections of pipe were removed, with minimal interruption of the water flow, for TOC, scanning electron microscopy, and biochemical analyses.

TOC. TOC was measured after scraping the microfouling film from 5-cm^2 rings of the prescored section of pipe; treatment with phosphoric acid to remove carbonates was followed by combustion with oxygen and measurement of CO_2 in a nondispersive infrared analyzer (Oceanography International Corp., College Station, Tex.) by R. Dyjak of Potomac Research, Inc., Panama City, Fla.

Scanning electron microscopy. Prescored coupons (1 cm^2), removed from the pipe without heat and with as little damage to the microfouling film as possible, were fixed in 0.075% (vol/vol) glutaraldehyde (Ladd Research Industries, Burlington, Vt.) in membrane-filtered (pore size, 0.4 μm; Millipore Corp., Bedford, Mass.) seawater at 4°C for 1 h. The coupons were then transferred to 3.3% (vol/vol) glutaraldehyde in filtered seawater for 1 h at 4°C. After this, they were swirled gently in filtered seawater or Instant Ocean made to the ionic strength of the natural seawater from which the samples were removed. This was repeated for a total of four washes. The coupons were then transferred to a 1.33% (wt/vol) solution of osmium tetroxide (Electron Microscopy Sciences, Fort Washington, Pa.) dissolved in 0.2 M sym-collidine buffer (Ladd Research Industries). The buffer was at pH 7.4, and the staining was for 1 h at 4°C. The coupons were then washed with four changes of filtered distilled water and dehydrated at room temperature in distilled water-ethyl alcohol (80:20 [vol/vol] for 10 min, 60:40 [vol/vol] for 10 min, 50:50 [vol/vol] for 10 min, and 30:70 [vol/vol] for 10 min). (At this point, the material can be held for several weeks as long as the surfaces remain covered by the 30:70 [vol/vol] distilled water-ethyl alcohol solution.)

When processing was continued, the dehydration proceeded by using distilled water-ethyl alcohol (20:80 [vol/vol] and 10:90 [vol/vol]) and three exposures each to 100% ethyl alcohol for 10 min at room temperature. The coupons were then placed in a critical point drier (built of stainless steel) and dried with CO_2 (1, 5). Once dried, the coupons were mounted on pedestals and coated with gold-palladium (60:40 [wt/wt]) to an approximate thickness of 10 nm in a Denton DV-502 rotary vacuum evaporator. The samples were then examined in the Cambridge Stereoscan S4-10 microscope at the magnifications given below.

Lipid extraction. Duplicate, 29-cm-long samples

TABLE 1. *Water characterization at the Naval Coastal Systems Center, Panama City, Fla., between 19 September and 5 December 1979*[a]

Day	Conductivity (S/cm)	Salinity (g/liter)	Temp (°C)	pH	Tide height (m)	Turbidity (NTU)[b]	Dissolved oxygen (mg/liter)	BOD (mg/ml)[b]	N-NH_3[b]	N-NO_3[b]	Phosphate (mg/liter)	TOC[b] (mg/liter)	Silicate (mg/liter)
0	43.6	27.7	27.5	8.1	0.43	1.0	5.7	0.9	0.04	0.03	0.03	3.4	0.90
8	40.0	24.4	24.5	8.2	0.49	1.2	6.0	0.7	0.08	0.06	0.01	3.2	0.63
15	38.4	24.7	26.3	8.0	0.37	1.1	4.2	0.7	0.10	0.05	0.022	3.7	0.72
21	34.4	22.9	23.8	8.0	0.06	1.3	7.1	1.7	0.02	0.07	0.014	4.7	0.75
28	25.4	19.8	16.1	7.8	0.34	1.3	6.3	1.3	0.04	0.05	0.012	5.3	0.36
35	32.3	26.0	16.0	8.1	0.06	1.5	6.5	0.9	0.02	0.03	0.006	3.8	0.15
42		30.0	23.0	8.2	0.31	1.5	6.7	1.2	<0.01	0.03	0.017	3.1	0.26
49	38.3	29.1	17.9	8.2	−0.03	1.4	7.6	1.1	<0.01	0.03	0.008	3.2	0.33
56	34.7	28.8	13.9	8.1	0.19	2.0	8.0	1.1	<0.01	0.02	0.008	2.7	0.26
63	39.3	29.3	19.1	8.1	−0.06	1.4	7.6	0.9	0.02	0.04	0.019	2.6	0.38
70	39.2	29.0	19.7	8.0	0.12	0.75	6.7	0.9	<0.01	0.03	0.004	2.5	0.22
77	33.7	29.3	11.7	8.1	−0.12	1.1	8.5	0.8	0.01	0.01	0.005	2.8	0.18

[a] Data reported by R. Dyjac of Potomac Research Inc., Panama City, Fla.

[b] Abbreviations: BOD, biological oxygen demand; N-NH_3, nitrogen as ammonia (mg of NH_3 per liter); N-NO_3, nitrogen as nitrate (mg of NO_3 per liter); TOC, total organic carbon.

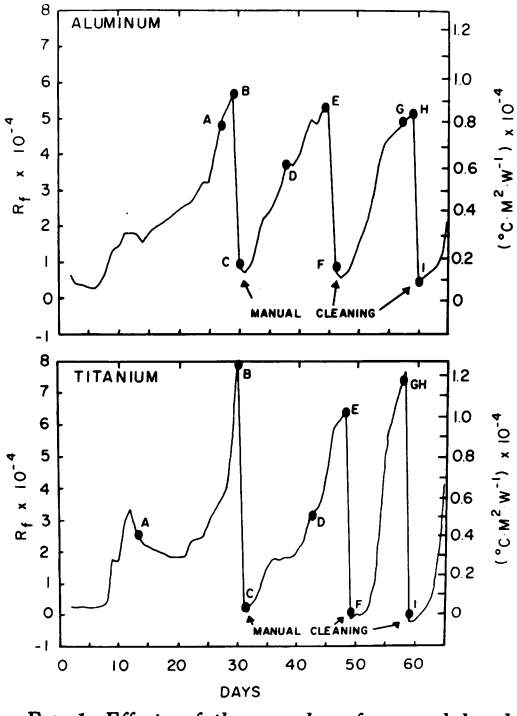

FIG. 1. *Effects of three cycles of manual brush cleaning with a stiff-bristle nylon brush on the heat transfer efficiency R_f, measured as (square feet × h × degrees Fahrenheit/British thermal units) × 10^{-4} for the left ordinate and as square meters × degrees centigrade per watt for the right ordinate, of 5052 aluminum (upper panel) and titanium (lower panel). Points indicated by letters indicate samples recovered for morphological and biochemical analysis.*

of pipe were removed, drained, purged with N_2, the ends capped with rubber stoppers, frozen in dry ice, and sent to the laboratory. There was no difference in the yield of extractable lipid phosphate from samples frozen and then extracted compared with those extracted immediately after removal from the flowing seawater. In the laboratory, the pipe sections were thawed and the ends were deburred and stoppered with a specially designed device (2), designed by John Highsmith of the Florida State University Biological Science Instrument shop, that forms a chloroform-tight Teflon seal to the metal inside the pipe. In essence, a stainless steel core is tightened to form the Teflon seal with the inside of the pipe. The method requires only the inside of the pipe to be deburred and the tube to be not far from round. For a 29-cm section of 2.66-cm diameter pipe, a total of 107 ml (28 ml of chloroform, 56 ml of methanol, and 23 ml of 10 mM phosphate buffer with 0.52 mM EDTA, pH 4.9) was added, and extraction was allowed to occur for 2 h at room temperature. At this time, a plug was removed and the solution was added to a 250-ml separatory funnel. Water and chloroform (28 ml of each) were added, and the solution was mixed and allowed to separate for 24 h. The chloroform phase was then filtered through fluted Whatman 2V filter paper and reduced in volume by evaporation under vacuum.

Phosphate analyses. A portion of the chloroform from the lipid extract was dried and digested with perchloric acid, and the amount of phosphate was determined colorimetrically as described (21).

Fatty acid analysis. The lipids were recovered from the chloroform phase, subjected to mild acid methanolysis, and fractionated by thin-layer chromatography. The fatty acid methyl ester band was recovered quantitatively from the silica gel and analyzed by gas-liquid chromatography as described (3).

Gas-liquid chromatography. The fatty acid methyl esters dissolved in hexane were introduced

without splitting by using a Varian model 8000 autosampler with a 30-s venting time on a 50-m glass capillary column coated with Silar 10C in a Varian 3700 gas chromatograph. The oven temperature was programmed from 42 to 192°C heating for 60 min at a rate of 2°C/min, followed by a 30-min isothermal period at 162°C, and final heating for 30 min at a rate of 1°C/min up to the maximum temperature of 192°C, which was maintained until the components were eluted. The helium carrier gas was at a flow rate of 1 ml/min, and the detection by flame ionization was at 225°C. The autosampler delivered 2 μl with no carryover between samples. A typical chromatogram is illustrated in Fig. 4. Fatty acid methyl esters were identified by comparing their elution volume on polar and nonpolar phases, before and after treatment with HBr or reduction with hydrogen, and by combined gas chromatography electron impact and chemical ionization mass spectrometry. These methods have been described previously (3).

Fatty acid nomenclature. The fatty acids are designated as the number of carbon atoms in a chain: the number of double bonds and the position of the ultimate double bond (the bond closest to the ω end of the molecule) designated as ω3, ω6, etc. The prefixed a, i, and Δ indicate anteiso, iso-branching, and cyclopropane ring, respectively.

Statistics. Analysis of variance and linear regression calculations were made by using a Radio Shack TRS-80 computer with the advanced statistical analysis 26-1705 program.

RESULTS

Change in heat transfer resistance with manual brush cleaning. Figure 1 shows the time course of three cycles of free fouling and cleaning for aluminum and titanium pipes. With each of the three cleanings, the rate of increase in heat transfer resistance increased. The time to reach a heat transfer resistance coefficient of 0.8×10^{-4} (°C × m²/watt) or 5.0×10^{-4} (ft² × h × °F/BTU) for aluminum was 27, 14, and 11 days for the first, second, and third cycles and 27, 13, and 5 days for titanium. Titanium showed increased heat transfer resistance more rapidly than aluminum.

Morphological effects of cleaning on the microfouling film. Before exposure to seawater, both the aluminum and titanium surfaces showed a clean surface with microscopic pits, and the surfaces were cleaned with detergent and thoroughly rinsed. With exposure to seawater, a morphologically complex community formed with sheets of filaments seen at low-power magnification and a complex assembly of organisms seen at high-power magnification on both aluminum and titanium. There was no striking or consistent difference between the morphologies of the first and third cycles on each metal (Fig. 2). The morphology seen under high-power magnification of microfouling film on both titanium and aluminum shows the diversity.

The morphology on aluminum of the residual microfouling community after cleaning shows a progressive colonization by web-like microbes on, in, and under the corrosion gel (Fig. 3Ca and Fa). Cleaning dislodged fragments of the gel, leaving the metallic surface with some residual microbial filaments. Cleaning of titanium left a residual detritus with few recognizable microbes (Fig. 3Ct and Ft).

Correlation of heat transfer resistance with microbial biomass measures. Comparisons of biomass measures and the heat transfer resistance coefficient (R_f), in terms of linear regression determination coefficients r^2, for aluminum and titanium were, respectively, 0.41 and 0.49 for total extractable palmitic acid, 0.78 and 0.75 for extractable lipid phosphate, 0.54 and 0.72 for total organic carbon, 0.43 and 0.28 for the TOC/total palmitic acid ratio, and 0.13 and 0.20 for the TOC/lipid phosphate ratio ($r^2 > 0.62$, $P < 0.01$). The only measure correlating significant heat transfer resistance on both metals appeared to be that of extractable lipid phosphate, which measures the phospholipids in the membranes of the microbes (21). However, these measures by themselves gave little insight into the community structure changes that might produce the increased rate of microfouling with cleaning shown in Fig. 1. Consequently, a suite of biochemical measurements was performed.

Differences in microbial biomass and community structure between the first and third cycles of free fouling. The biomass and community structure of the free-fouling microbiota formed in the first and third cycles (Fig. 1, points B and H) of free fouling on both aluminum and titanium are given in Table 2. On aluminum, there was a significant increase in the total a + i 15:0 and the proportions of a + i 15:0/15:0 and 18:1ω7/16:0 between the first and third cycles. On titanium, there was a significant increase in total polyenoic fatty acids longer than 20 carbons and in the proportion of Δ17:0 + Δ19:0/16:0. There was a decrease in the amount of cyclopropane fatty acid Δ17:0 and in the proportions of 18:1ω7/18:1ω9 and 18:2ω6/16:0 between the first and third cycles.

Comparison of the free-fouling films on titanium and aluminum. The biomass and community structure of the free-fouling community formed after free fouling to approximately the same level of heat transfer resistance in the second cycle on titanium and aluminum exhibited significant differences (Table 3, aluminum E versus titanium E). The film from titanium had significantly higher absolute amounts of lipid phosphate and a + i 15:0 and

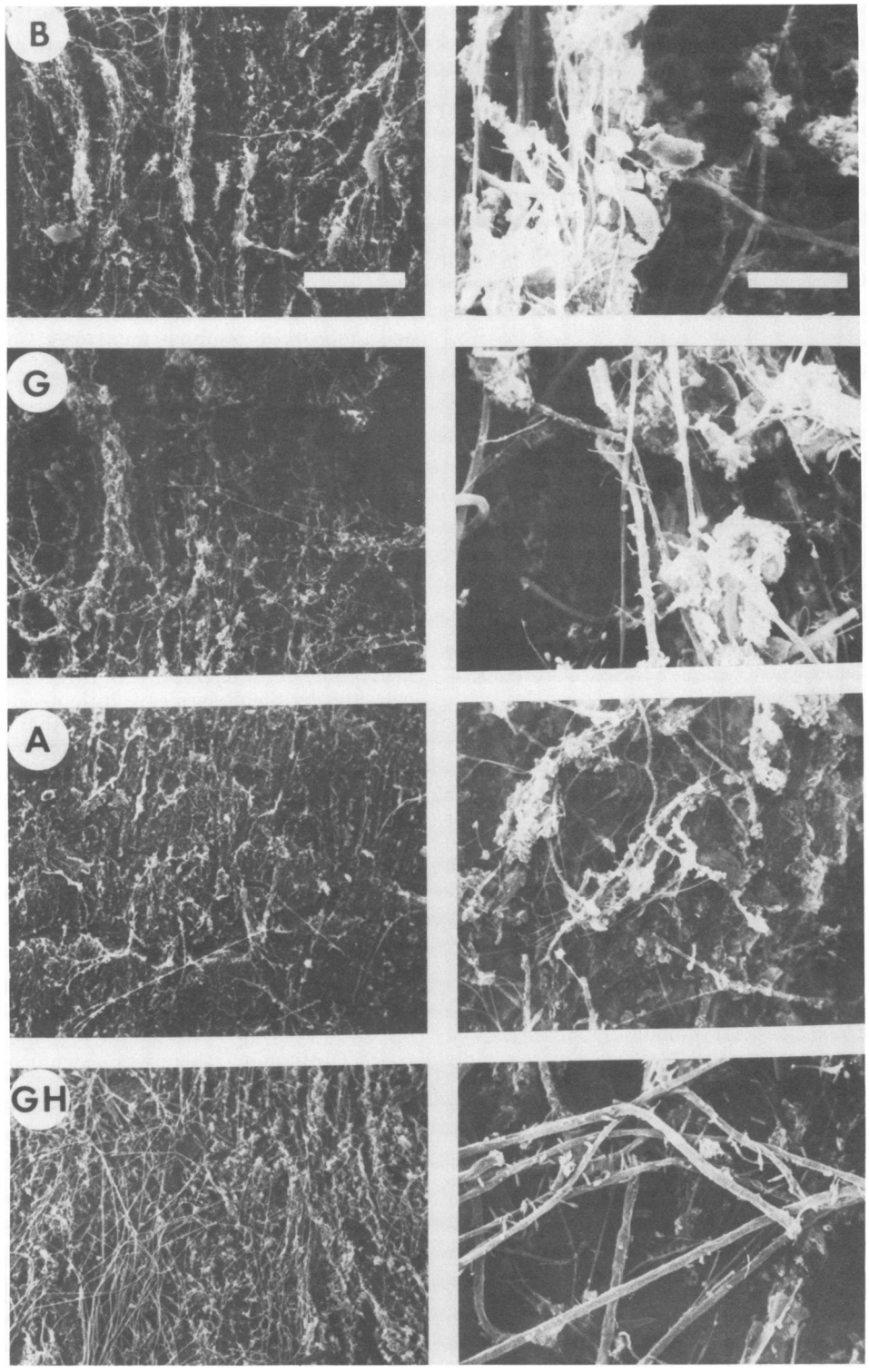

FIG. 2. *Scanning electron micrograph of the microfouling film formed after free fouling on aluminum in the first (B) and third (G) cycles and on titanium in the first (A) and third (GH) cycles. (Letters designate Fig. 1 sampling points.) Left-hand column magnification, 210-fold; bar, 100 μm. Right-hand column magnification, 2,100-fold; bar, 10 μm.*

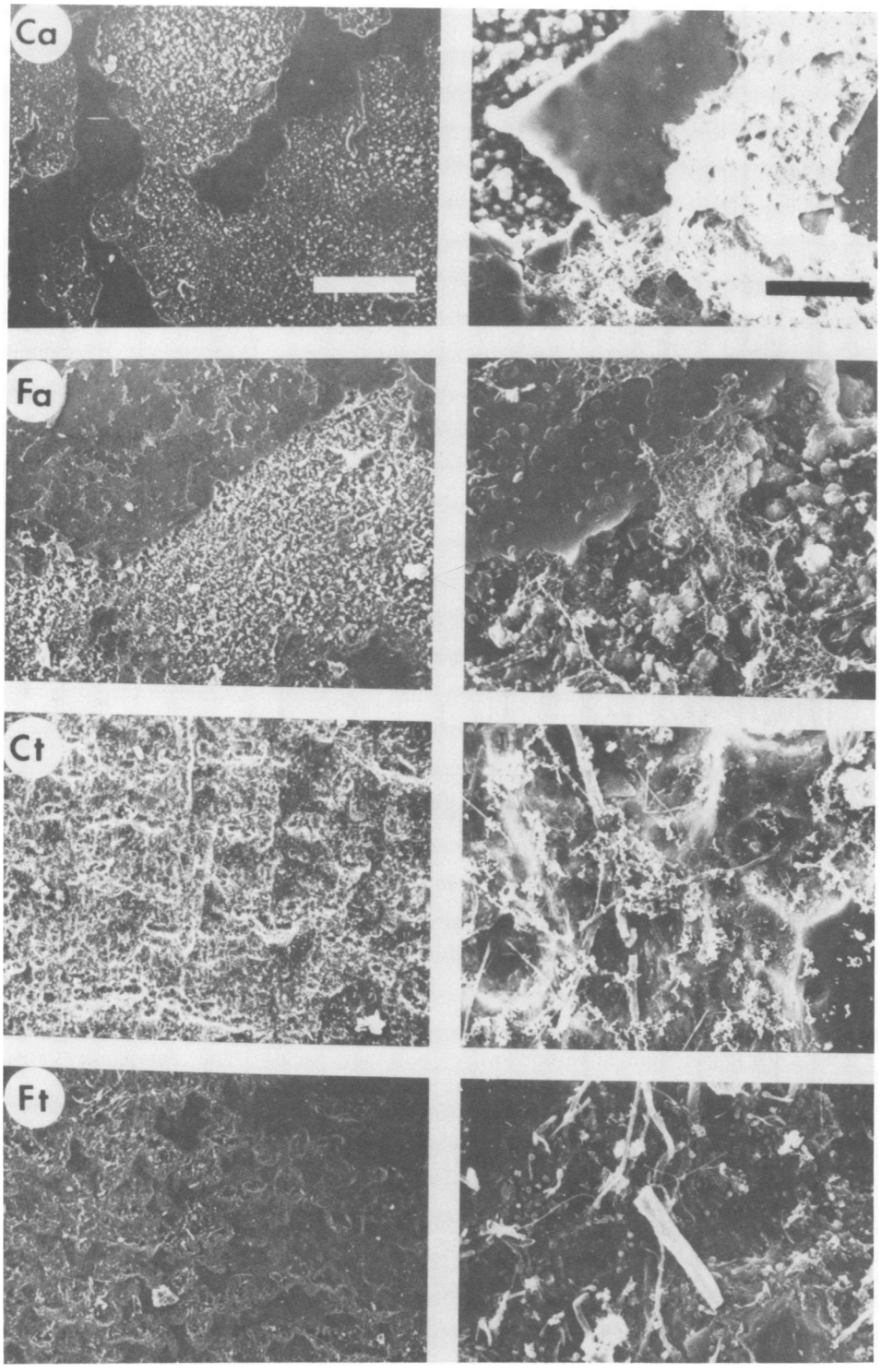

FIG. 3. *Scanning electron micrograph of the microfouling film after manual cleaning of aluminum (a) after the first (C) and second (F) cycles and titanium (t) after the first (C) and second (F) cycles. Left-hand column magnification, 210-fold; bar, 100 μm. Right-hand column magnification, 2,100-fold; bar, 10 μm.*

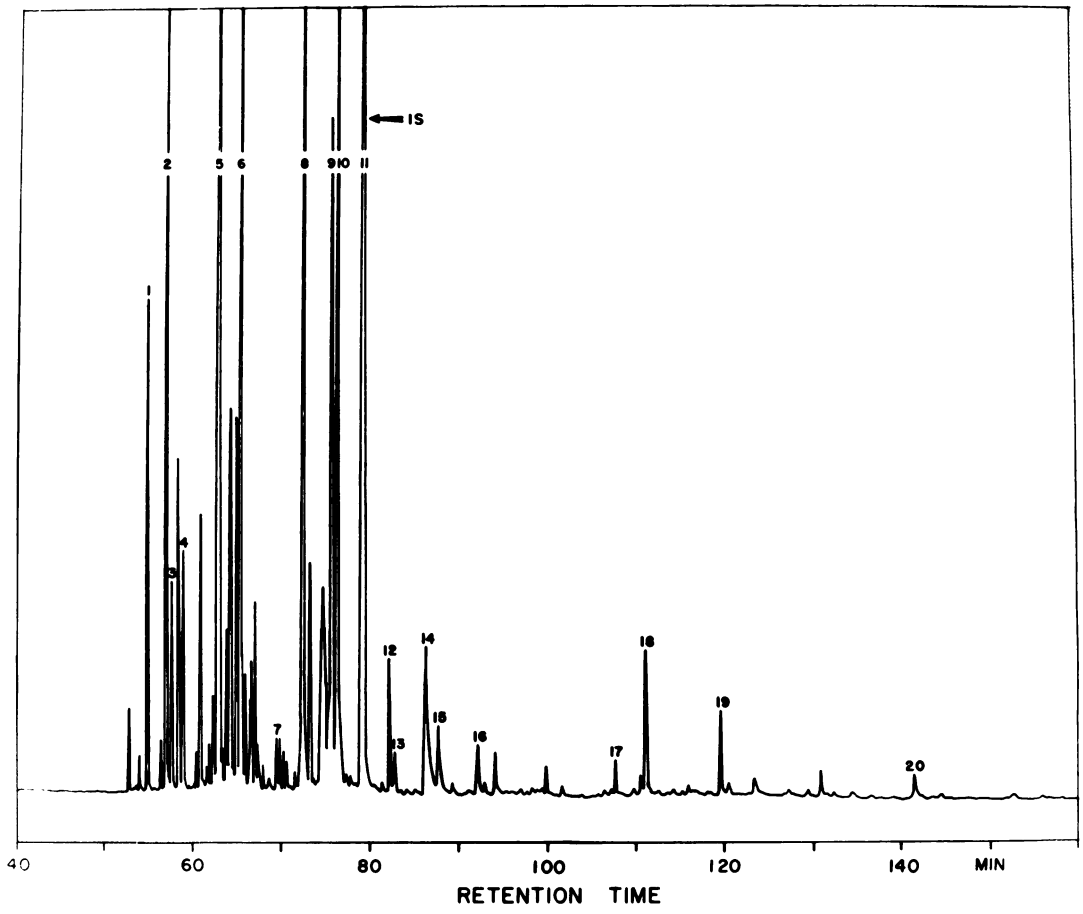

FIG. 4. *Gas chromatogram of fatty acid methyl esters of the lipids extracted from the microfouling community separated on a 50-m Silar 10C glass capillary column from the sample at A in Figure 1, top panel. Components used were 14:0 (1), i15:0 (2), a15:0 (3), 15:0 (4), 16:0 (5), 16:1ω7 (6), Δ17:0 (7), 18:0 (8), 18:1ω9 (9), 18:1ω7 (10), 19:0 IS (11), 18:2ω6 (12), Δ19:0 (13), 18:3ω6 (14), 20:0 (15), 18:3ω3 (16), 22:0 (17), 20:4ω6 (18), 20:5ω3 (19), 22:6ω3 (20).*

relative amounts of a + i 15:0/15:0 and a + i 15:0/16:0, 18:1ω7/18:1ω9 and in the ratio of polyenoic fatty acids longer than 20 carbons with ω6 unsaturation compared with ω3 unsaturation. The microfouling film formed on aluminum during the second cycle had a significantly higher proportion of 18:2ω6/16:0 and total polyenoic fatty acids longer than 20 carbon atoms.

Effect of cleaning on the microbial biomass and community structure. After free fouling, cleaning aluminum and titanium pipes with the stiff-bristle nylon brush decreased the heat transfer resistance (Fig. 1, points C, F, and I).

On the aluminum surface, comparison of the biomass of the free-fouling microbial assembly (Table 3, point E) to the residual community after the second cleaning cycle (Table 3, points I and F) showed a significant decrease in the lipid phosphate, TOC, a + i 15:0, and total polyenoic acids. The community structure showed decreases in the proportions of a + i 15:0/15:0, a + i 15:0/16:0, Δ17:0 + Δ19:0/16:0, 18:1ω7/16:0, 18:1ω7/18:1ω9, and the total polyenoic fatty acids longer than 20 carbon atoms/16:0. On titanium, all biochemical markers listed in Table 3 significantly decreased except the absolute amount of 18:1ω7 and the proportions of Δ17:0 + Δ19:0/16:0 and 18:2ω6/16:0.

Differences between the residual communities left after the first and third cycles of cleaning. After cleaning titanium, the residual community left between the first and third cycles showed an increase in the lipid phosphate, total palmitic acid, 18:1ω7, and the proportions of 18:1ω7/16:0 and 18:1ω7/18:1ω9. There were

TABLE 2. *Biomass and community structure differences between the microfouling film forming on aluminum and titanium pipes between the first and third cycles of free fouling with manual cleaning*[a]

Biochemical marker	Aluminum		Titanium	
	Cycle 1 (B)	Cycle 3 (H)	Cycle 1 (B)	Cycle 3 (G)
Biomass				
R_f	5.67	5.15	8.56	7.63
Lipid phosphate[b]	3.44 (1.88)	2.97 (0.78)	5.36 (2.72)	3.50 (0.15)
TOC[c]	34.8 (1.7)	38.2 (2.48)^{xx}	49.7 (16.7)	29.5 (4.5)
Total palmitic acid[d]	0.55 (0.06)	0.68 (0.10)	0.65 (0.02)	1.32 (0.6)
Total a + i 15:0	0.15 (0.05)	0.42 (0.17)^{x}	0.09 (0.05)	0.05 (0.02)
Total Δ17:0	0.02 (0.00)	0.03 (0.03)	0.04 (0.02)	0.008 (0.002)^{y}
Total 18:1ω7	0.14 (0.07)	0.16 (0.04)	0.19 (0.09)	1.7 (2.2)
Total 18:2ω6	0.04 (0.00)	0.031 (0.006)	0.07 (0.04)	0.03 (0.004)
Total polyenoics >20	0.13 (0.07)	0.23 (0.11)	0.17 (0.07)	0.51 (0.12)^{yy}
Community structure				
a + i 15:0/15:0	0.26 (0.06)	0.58 (0.05)^{xx}	4.4 (0.3)	5.4 (0.1)
a + i 15:0/16:0	4.69 (0.89)	4.22 (0.38)	0.38 (0.08)	0.38 (0.2)
Δ17:0 + Δ19:0/16:0	0.05 (0.004)	0.08 (0.09)	0.07 (0.006)	0.11 (0.003)^{yyy}
18:1ω7/16:0	0.70 (0.07)	1.02 (0.19)^{x}	0.79 (0.03)	0.79 (0.3)
18:1ω7/18:1ω9	3.02 (1.40)	4.43 (1.13)	4.25 (0.4)	2.64 (0.3)^{yy}
18:2ω6/16:0	0.06 (0.00)	0.05 (0.02)	0.07 (0.002)	0.05 (0.01)^{yyy}
Total polyenoics >20/16:0	0.25 (0.15)	0.36 (0.22)	0.26 (0.12)	0.33 (0.01)
Polyenoics ω6/ω3	0.89 (0.42)	0.63 (0.29)	0.78 (0.15)	0.40 (0.06)

[a] B, G, and H refer to samples taken as indicated in Fig. 1. Data are expressed as the $\bar{x}$ (± standard deviation), except as otherwise indicated. Superscripts of one, two, and three letters indicate, respectively, significant differences between means, as determined by one-way analysis of variance, at the 0.1, 0.05, and 0.01 levels within B-H aluminum (x) and B-G titanium (y).

[b] Data expressed in nanomoles of lipid phosphate per square centimeter.

[c] Data expressed in nanograms of carbon per square centimeter.

[d] Data expressed in nanomoles per square centimeter; $\bar{x}$ (standard deviation) for all fatty acids.

significant decreases between the proportions of Δ17:0 + Δ19:0/16:0 and 18:2ω6/16:0 (Table 4). There were no significant differences between the residual microbial components after the first and third cleaning on aluminum.

Comparison of the residual communities on aluminum and titanium. The residual communities left after cleaning the second cycle of fouling are given in Table 3 (aluminum F versus titanium F). The residual film on titanium compared to aluminum had significantly more total lipid phosphate and greater absolute amounts of a + i 15:0 and relative proportions of a + i 15:0/15:0, a + i 15:0/16:0, Δ17:0 + Δ19/16:0, 18:1ω7/16:0, and 18:1ω7/18:1ω9. In addition, there were significant increases in both the absolute and relative amounts of total polyenoic fatty acids longer than 20 carbon atoms.

The residual communities left after the third cycle of cleaning of titanium and aluminum showed fewer significant differences.

Extracellular polymer formation and microfouling. The residual microfouling communities remaining after 20 passes of the nylon brush on the aluminum yielded higher heat transfer resistance (R_f = 0.67 [0.20], $\bar{x}$ [standard deviation]) than titanium (R_f = 0.26 [0.26]), significantly (P = 0.005) lower biomass, measured as extractable lipid phosphate, 0.21 (0.05) nmol/cm^2 for aluminum versus 0.45 (0.17) nmol/cm^2 for titanium.

With TOC used as a measure of the total biomass and lipid phosphate used as a measure of the cellular biomass, the TOC/lipid phosphate ratio can be considered as a measure of the "extracellular biomass" (21). The residual communities on both aluminum and titanium contained two to three times the extracellular biomass of the free-fouling communities, and the residual community left on aluminum had significantly more extracellular biomass than the community left on titanium (Table 5). The extracellular polymer binding a filamentous bacterium to the aluminum surface can be seen in Fig. 5.

DISCUSSION

Effect of brushing. To maintain an economically feasible ocean thermal energy conversion system, the heat transfer resistance must be maintained at a low level (<5.0 × 10^{-4} [ft^2 × h × °F/BTU] [9]). Maintenance of a low heat transfer resistance requires cleaning, so quantitative methods were applied to define the

TABLE 3. *Biomass and community structure of the microfouling community on aluminum and titanium pipes before and after the second cleaning cycle*[a]

Biochemical marker	Aluminum		Titanium		Significance	
	E	F	E	F	Aluminum E vs titanium E	Aluminum F vs titanium F
Biomass						
R_f	5.31	0.73	6.53	0.52		
Lipid phosphate[b]	3.44 (0.05)	0.21 (0.00)^{www}	5.18 (0.26)	0.50 (0.04)^{xxx}	yyy	zzz
TOC[c]	49.3 (5.51)	7.00 (2.3)^{www}	53.5 (9.3)	6.14 (3.03)^{xx}		
Total palmitic acid[d]	0.45 (0.70)	0.18 (0.24)	0.74 (0.22)	0.16 (0.01)^{xx}		
Total a + i 15:0	014 (0.00)	0.005 (0.004)^{www}	0.26 (0.04)	0.013 (0.001)^{xxx}	yyy	z
Total 15:0	0.04 (0.001)	0.022 (0.024)^{www}	0.07 (0.02)	0.016 (0.004)^{xx}		
Total Δ17:0	0.02 (0.003)	0.05 (0.02)	0.023 (0.003)	0.008 (0.001)^{xx}		
Total 18:1ω7	0.14 (0.005)	0.34 (0.37)	0.2 (0.01)	0.16 (0.05)		
Total 18:2ω6	0.05 (0.006)	0.17 (0.23)	0.05 (0.01)	0.01 (0.007)^{xx}		
Total polyenoics >20	0.40 (0.07)	0.012 (0.004)^{www}	0.38 (0.03)	0.073 (0.0007)^{xxx}		zz
Community structure						
a + i 15:0/15:0	3.18 (0.18)	0.69 (0.23)^{www}	4.02 (0.32)	1.41 (1.01)^{xxx}	yy	zz
a + i 15:0/16:0	0.27 (0.02)	0.04 (0.01)^{www}	0.37 (0.05)	0.14 (0.02)^{xx}	y	zzz
Δ17:0 + Δ19:0/16:0	0.08 (0.02)	0.04 (0.02)^{w}	0.06 (0.02)	0.09 (0.03)		z
18:1ω7/16:0	0.88 (0.04)	0.14 (0.06)^{www}	1.08 (0.29)	0.52 (0.12)^{x}		zz
18:1ω7/18:1ω9	3.30 (0.10)	0.16 (0.09)^{www}	3.77 (0.18)	0.59 (0.29)^{xxx}	yy	z
18:2ω6/16:0	0.10 (0.02)	0.30 (0.30)	0.067 (0.007)	0.07 (0.04)	y	
Total polyenoics >20/16:0	0.77 (0.09)	0.06 (0.05)^{www}	0.55 (0.20)	0.17 (0.04)^{x}	y	zz
Polyenoic ω6/ω3	0.32 (0.004)		0.39 (0.01)	0.49 (0.22)	yyy	

[a] E and F refer to samples taken as indicated in Fig. 1. Data are expressed as the $\bar{x}$ (± standard deviation), except as otherwise indicated. Superscripts of one, two, and three letters indicate, respectively, significant differences between the means, as determined by one-way analysis of variance, at the 0.1, 0.05, and 0.01 levels within E-F aluminum (w) and E-F titanium (x) and between aluminum E versus titanium E (y) and aluminum F versus titanium F (z).

[b] Data expressed in nanomoles of lipid phosphate per square centimeter.

[c] Data expressed as nanograms of carbon per square centimeter.

[d] Data expressed as nanomoles per square centimeter; $\bar{x}$ (± standard deviation) for all fatty acids.

TABLE 4. *Biomass and community structure differences between the residual communities left after manual cleaning between the first and third cleaning of titanium and aluminum pipes*[a]

Biochemical marker	Titanium		Aluminum cycle 3 (I)
	Cycle 1 (C)	Cycle 3 (I)	
Biomass			
R_f	0.24	0.01	0.45
Lipid phosphate[b]	0.26 (0.21)	0.56	0.16 (0.16)^{yy}
Total palmitic acid[c]	0.24 (0.007)	0.63 (0.26)^{x}	0.27 (0.15)
Total a + i 15:0	0.018 (0.005)	0.072 (0.05)	0.02 (0.03)
Total 15:0	0.015 (0.002)	0.028 (0.006)	0.06 (0.07)
Total Δ17:0	0.008 (0.001)	0.008 (0.003)	0.01 (0.001)
Total 18:1ω7	0.07 (0.01)	0.16 (0.06)^{x}	0.14 (0.12)
Total 18:2ω6	0.016 (0.0007)	0.03 (0.01)	0.014 (0.013)
Total 24:0	0.03 (0.03)	0.024 (0.01)	
Total polyenoics >20	0.017 (0.017)	0.11 (0.14)	0.049 (0.056)
Community structure			
a + i 15:0/15:0	1.26 (0.06)	2.82 (1.6)	0.72 (0.53)
a + i 15:0/16:0	0.08 (0.01)	0.12 (0.05)	0.09 (0.09)
Δ17:0 + Δ19:0/16:0	0.06 (0.001)	0.02 (0.006)^{xxx}	0.04 (0.06)
18:1ω7/16:0	0.14 (0.01)	0.31 (0.035)^{xx}	0.17 (0.05)^{yy}
18:1ω7/18:1ω9	0.49 (0.02)	1.18 (0.22)^{xx}	0.39 (0.05)^{yy}
18:2ω6/16:0	0.07 (0.001)	0.05 (0.001)^{xxx}	0.04 (0.03)
Total polyenoics >20/16:0	0.074 (0.07)	0.14 (0.16)	0.11 (0.08)
Polyenoic ω6/ω3	1.19 (0.44)	0.41	0.94 (0.00)

[a] C and I refer to samples taken as indicated in Fig. 1. Data are expressed as the $\bar{x}$ (± standard deviation). Superscripts of one, two, and three letters indicate, respectively, significant differences between the means, as determined by one-way analysis of variance, at the 0.1, 0.05, and 0.01 levels between cycles 1 and 3 titanium (x) and between cycle 3 aluminum and titanium (y).

[b] Data given as nanomoles of lipid phosphate per square centimeter.

[c] Data expressed as nanomoles per square centimeter; $\bar{x}$ (± standard deviation) for all fatty acids.

changes in the microbial fouling film. The results of three cycles of free fouling with manual brush cleaning to decrease heat transfer resistance resulted in a residual microbial community that stimulated a faster rate of fouling on both metals (Fig. 1). The free fouling on titanium was faster with each cycle (Fig. 1), and the residual community was richer in bacteria and cellular biomass but lower in heat transfer resistance than was the residual community on aluminum with its high level of extracellular polymer plaque.

TABLE 5. *Extracellular polymer formation in titanium and aluminum in the free-fouling and residue microfouling films*[a]

Metal	Free fouling (A, B, D, E, G, H)[b]	Residue (C, F)[c]
Titanium	9.2 (0.74)$^{vv, www, z}$	16.7 (6.2)$^{vv, xx}$
Aluminum	11.1 (2.57)$^{xx, yyy, z}$	28 (7.1)$^{www, yyy}$

[a] Letters A through H refer to samples taken as indicated in Fig. 1. Data are expressed as the $\bar{x}$ (± standard deviation) in nanograms of TOC per nanomoles of lipid phosphate. Superscripts of one, two, and three letters indicate, respectively, statistical significance, as determined by one-way analysis of variance, at the 0.1, 0.05, and 0.01 levels for the following: titanium free fouling versus titanium residue (v), titanium free fouling versus aluminum residue (w); aluminum free fouling versus titanium residue (x); aluminum free fouling versus aluminum residue (y); and titanium free fouling versus aluminum free fouling (z).

[b] For $\bar{x}$ (± standard deviation), $n = 12$.

[c] For $\bar{x}$ (± standard deviation), $n = 4$.

Interpretation of the lipid measures of biomass and community structure. A summary of the biomass and community structure measures used in this study is given in Table 6.

With cycles of cleaning, the free-fouling microbial film formed on aluminum became enriched in bacteria containing the short-branched fatty acids (Table 2). On titanium, repeated cycles of free fouling induced a greater microeucaryotic biomass as reflected in the recoverable polyenoic fatty acids (Table 2). The shifts in free-fouling communities on both metals could be the results of changes in nutrients or temperature, the results of cleaning and refouling, or both (Fig. 1; Tables 1 and 2). Irrespective of the cause, titanium fouled more rapidly and to a greater extent than aluminum (Fig. 1; Table 2). Comparison of the microfouling films on aluminum and titanium that have the same resistance to heat transfer shows significantly higher lipid phosphate and total short-branched fatty acids from bacteria in the film from titanium pipes (Table 3).

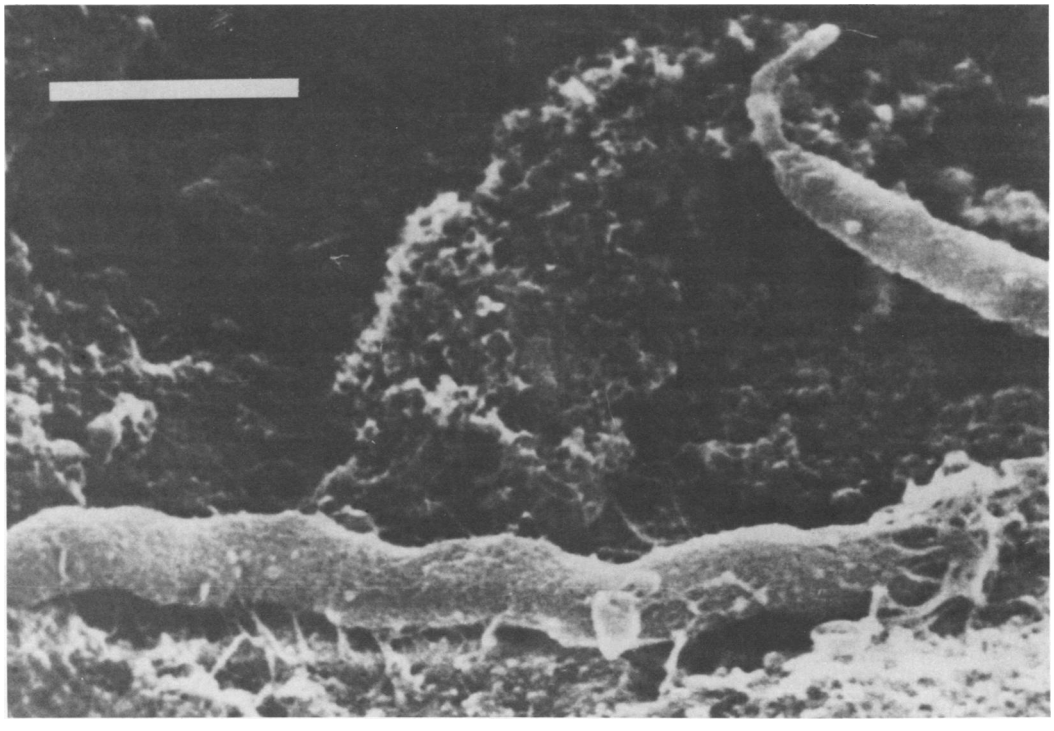

FIG. 5. *Scanning electron micrograph of bacteria on an aluminum surface showing the extracellular binding material. Magnification, 21,000-fold; bar, 1 μm.*

TABLE 6. *Summary of biochemical measures[a] of microfouling biomass and community structure*

Biochemical marker	Measures
Biomass	
Lipid phosphate	Phospholipid; total "membranes" biomass
Total palmitic acid	Total lipid; membrane plus triglyceride biomass
TOC	Total mass; exopolymer plus cellular carbon
Total a + i 15:0	Bacteria; a measure of some bacteria
Total 15:0	Bacteria; one component of the bacteria
Total Δ17:0	Bacteria; another component of the bacteria forming cyclopropane fatty acids
Total 18:1ω7	Bacteria; a third component of the bacteria with the anaerobic desaturation pathway
Total 18:2ω6	Linoleic acid; filamentous bacteria, blue-green algae (cyanobacteria), fungi
Total polyenoics >20	Microeucaryotes; protozoa, fungi, algae
Total 24:0	Long straight chain; microeucaryotes
Community structure	
a + i 15:0/15:0	Proportion of total bacteria on one type
a + i 15:0/16:0	Proportion of that type of bacteria in the total microfouling organisms
Δ17:0 + Δ19:0/16:0	Proportion of the second type of bacteria in the total microfouling community
18:1ω7/16:0	Proportion of third type of bacteria in the total microfouling community
18:1ω7/18:1ω9	Proportion of third type of bacteria in the portion of the community containing oleic acid (bacteria and microeucaryotes)
18:2ω6/16:0	Proportion of filamentous, gliding or blue-green algae in the total film
Total polyenoics >20/16:0	Proportion of the total microeucaryotes in the total film
Polyenoic ω6/ω3	Proportion of protozoa (animals) to algae, diatoms, fungi (plants) in the microeucaryotes

[a] Justification for these measures is given in references 7, 17, 18, 20–22.

Manual cleaning with the stiff-bristle nylon brush decreased the absolute amount of all components except as follows: the total palmitic acid, cyclopropane and *cis*-vaccenic fatty acids from bacteria and the linoleic acid (18:2ω6) found in some bacteria, fungi, and algae in the film on aluminum or in bacteria containing the anaerobic desaturating pathway producing *cis*-vaccenic acid (18:1ω7) in the film from titanium. In comparison with aluminum, brushing left films on titanium that were more enriched in absolute amounts of bacteria containing branched fatty acids and microeucaryotes containing polyenoic fatty acids and that had significantly different proportions of nearly all components than films remaining on aluminum (Table 3).

With successive cycles of brushing, the residual community on titanium showed twofold increases in membrane biomass and in the bacteria containing short branched fatty acids (a + i 15:0), the anaerobic pathway (18:1ω6), and microeucaryotes, but decreases in the relative proportions of bacterial cyclopropane fatty acid (Δ17:0 + Δ19:0) and organisms containing linoleic acid (18:2ω7) (Table 4). Three cycles of cleaning induced no significant change in the biomass and community structure of the residual microbial assembly on aluminum. When compared to the residue on aluminum, the residual communities on titanium contained twofold more membrane biomass and microeucaryotes with a bacterial population relatively enriched in all components but particularly in the components forming the short-branched fatty acids (Tables 3 and 4). There were differences in the community structure in the residual film on aluminum and titanium, and the richness of the residual bacterial communities on titanium may be the inoculum for the faster fouling rates. Repeated cycles of manual brush cleaning selected a residual microfouling community enriched in bacteria that utilized the anaerobic pathway of desaturation on both aluminum and titanium and formed a film that stimulated the rate of free fouling by both bacteria and microeucaryotes.

Formation of extracellular polymers. Continued cleaning cycles over the long periods necessary for the viability of an ocean thermal energy conversion plant could select for an increasingly resistant microbial fouling community. Three cycles of cleaning in the enriched coastal waters of this experiment selected a population with twofold higher proportions of extracellular polymer measured as the TOC/lipid phosphate ratio on both aluminum and titanium surfaces (Table 5). The extracellular polymer can be detected morphologically in scanning electron microscopy (Fig. 5).

The chemical nature of this extracellular polymer, the measurements of microbial metabolic activities by incorporation and turnover of ^{13}C-labeled precursors by gas chromatography-mass spectrometry, and the application of additional biochemical measures of community structure are the future goals of this research.

ACKNOWLEDGMENTS

This work was supported by contract 31-109-38-4502 from the Department of Energy (Argonne National Laboratory, Argonne, Illinois), grants OCE 76-19671 and DEB-7818401 from the National Science Foundation, and grant 04-7-158-4406 from the National Oceanic and Atmospheric Administration Office of Sea Grant, Department of Commerce.

G. F. Popper and A. P. Gavin of the Argonne National Laboratory administered the ocean thermal energy conversion simulation facility. R. Dyjak of Potomac Research, Inc., Panama City, Fla., recovered the samples and performed the site characterization and TOC analyses. Scanning electron micrographs were prepared by W. I. Miller III, Florida State University, and some of the biochemical analyses were performed by J. H. Parker and G. A. Smith of this laboratory.

LITERATURE CITED

1. **Anderson, T. F.** 1951. Techniques for the preservation of three-dimensional structure in preparing specimens for the electron microscope. Trans. N.Y. Acad. Sci. **13**:130–134.
2. **Bobbie, R. J., J. S. Nickels, W. M. Davis, D. C. White, D. F. Lott, R. Dyjak, and J. Hollwell.** 1979. Measurement of microfouling mass and community structure during succession in OTEC simulators—a preliminary report, p. 101–120. *In* Proceedings of the ocean thermal energy conversion (OTEC) biofouling, corrosion, and materials workshop. Argonne National Laboratory, Argonne, Ill.
3. **Bobbie, R. J., and D. C. White.** 1980. Characterization of benthic microbial community structure by high-resolution gas chromatography of fatty acid methyl esters. Appl. Environ. Microbiol. **39**:1212–1222.
4. **Braswell, J. A., D. F. Lott, and S. M. Hedlicka.** 1979. Preliminary evaluation of flow-driven brushes for removal of soft biofouling from heat exchanger tubes in OTEC power plants, p. 149–162. *In* Proceedings of the ocean thermal energy conversion (OTEC) biofouling, corrosion and materials workshop. Argonne National Laboratory, Argonne, Ill.
5. **Cohen, A. L.** 1974. Critical point drying, p. 44–112. *In* Principles and techniques of scanning electron microscopy, vol. 1. Van Nostrand Reinhold Co., New York.
6. **Corpe, W. A.** 1970. An acid polysaccharide produced by a primary film-forming marine bacterium, p. 402–412. *In* C. J. Corum (ed.), Developments in industrial microbiology, vol. 11. American Institute for Biological Sciences, Washington, D.C.
7. **Corpe, W. A.** 1972. Microfouling: the role of primary film forming marine bacteria, p. 598–609. *In* R. F. Acker (ed.), Proceedings of Third International Congress of Marine Corrosion and Microfouling. Northwestern University Press, Evanston, Ill.
8. **Davis, W. M., and D. C. White.** 1980. Fluorometric determination of adenosine nucleotide derivatives as measures of the microfouling, detrital and sedimentary microbial biomass and physiological status. Appl. Environ. Microbiol. **40**:539–548.
9. **Kinelski, E. H.** 1979. The requirements for biofouling, corrosion, and materials in the OTEC program, p. 3–12. *In* Proceedings of the ocean thermal energy conversion (OTEC) biofouling, corrosion, and materials workshop. Argonne National Laboratory, Argonne, Ill.
10. **Loeb, G. I., and R. A. Neuhof.** 1973. Marine conditioning films. Adv. Chem. Ser. **145**:319–335.
11. **Lott, D. F.** 1980. In-situ cleaning of OTEC heat exchangers, p. IIE/4-1-IIE/4-15. *In* Expanded abstracts of the 7th ocean energy conference, Washington, D.C.
12. **Marshall, K. C.** 1972. Mechanism of adhesion of marine bacteria to surfaces, p. 625–632. *In* R. F. Acker (ed.), Proceedings of Third International Congress of Marine Corrosion and Microfouling. Northwestern University Press, Evanston, Ill.
13. **Marshall, K. C.** 1976. Interfaces in microbial ecology. Harvard University Press, Cambridge, Mass.
14. **Marshall, K. C., R. Stout, and R. Mitchell.** 1971. Selective sorption of bacteria from seawater. Can. J. Microbiol. **17**:1413–1416.
15. **Marshall, K. C., R. Stout, and R. Mitchell.** 1971. Mechanism of the initial events in the sorption of marine bacteria to surfaces. J. Gen. Microbiol. **68**:337–348.
16. **Marszalek, D. S., S. M. Gerchakov, and L. R. Udey.** 1979. Influence of substrate composition on marine microfouling. Appl. Environ. Microbiol. **38**:987–995.
17. **White, D. C., R. J. Bobbie, J. S. Herron, J. D. King, and S. J. Morrison.** 1979. Biochemical measurements of microbial mass and activity from environmental samples, p. 69–81. *In* J. W. Costerton and R. R. Colwell (ed.), Native aquatic bacteria: enumeration, activity and ecology, ASTM STP 695. American Society for Testing and Materials, Philadelphia.
18. **White, D. C., R. J. Bobbie, J. D. King, J. S. Nickels, and P. Amoe.** 1979. Lipid analysis of sediments for microbial biomass and community structure, p. 87–103. *In* C. D. Litchfield and P. L. Seyfried (ed.), Methodology for biomass determinations and microbial activities in sediments, ASTP STP 673. American Society for Testing and Materials, Philadelphia.
19. **White, D. C., R. J. Bobbie, S. J. Morrison, D. K. Oosterhof, C. W. Taylor, and D. A. Meeter.** 1977. Determination of microbial activity of estuarine detritus by relative rates of lipid biosynthesis. Limnol. Oceanogr. **22**:1089–1099.
20. **White, D. C., R. J. Bobbie, J. S. Nickels, S. D. Fazio, and W. M. Davis.** 1980. Non-selective biochemical methods for the determination of fungal mass and community structure in estuarine detrital microflora. Bot. Mar. **23**:239–250.
21. **White, D. C., W. M. Davis, J. S. Nickels, J. D. King, and R. J. Bobbie.** 1979. Determination of the sedimentary microbial biomass by extractible lipid phosphate. Oecologia **40**:51–62.
22. **White, D. C., R. H. Findlay, S. D. Fazio, R. J. Bobbie, J. S. Nickels, W. M. Davis, G. A. Smith, and R. F. Martz.** 1980. Effects of bioturbation and predation by *Mellita quinquiesperforata* on the sedimentary microbial community structure, p. 163–171. *In* V. S. Kennedy (ed.), Estuarine perspectives. Academic Press, Inc., New York.
23. **White, D. C., R. J. Livingston, R. J. Bobbie, and J. S. Nickels.** 1979. Effects of surface composition, water column chemistry, and time of exposure on the composition of the detrital microflora and associated macrofauna in Apalachicola Bay, Florida, p. 83–116. *In* R. J. Livingston (ed.), Ecological processes in coastal and marine systems. Plenum Publishing Corp., New York.
24. **Young, L. Y., and R. Mitchell.** 1972. The role of chemotactic responses in primary microbial film formation, p. 617–624. *In* R. F. Acker (ed.), Proceedings of Third International Congress of Marine Corrosion and Microfouling. Northwestern University Press, Evanston, Ill.